Available online at www.sciencedirect.com

ScienceDirect

Physics Procedia 61 (2015) 232 – 240

Physics Procedia

The MAJORANA DEMONSTRATOR for $0\nu\beta\beta$: Current Status and Future Plans

M.P. Green[a], N. Abgrall[b], E. Aguayo[c], F.T. Avignone III[d,a], A.S. Barabash[e], F.E. Bertrand[a], M. Boswell[f], V. Brudanin[g], M. Busch[h,i], D. Byram[j], A.S. Caldwell[k], Y-D. Chan[b], C.D. Christofferson[k], D.C. Combs[l,i], C. Cuesta[m], J.A. Detwiler[m], P.J. Doe[m], Yu. Efremenko[n], V. Egorov[g], H. Ejiri[o], S.R. Elliott[f], J.E. Fast[c], P. Finnerty[p,i], F.M. Fraenkle[p,i], A. Galindo-Uribarri[a], G.K. Giovanetti[p,i], J. Goett[f], J. Gruszko[m], V.E. Guiseppe[d], K. Gusev[g], A.L. Hallin[q], R. Hazama[o], A. Hegai[b,1], R. Henning[p,i], E.W. Hoppe[c], S. Howard[k], M.A. Howe[p,i], K.J. Keeter[r], M.F. Kidd[s], O. Kochetov[g], S.I. Konovalov[e], R.T. Kouzes[c], B.D. LaFerriere[c], J. Leon[m], L.E. Leviner[l,i], J.C. Loach[t], J. MacMullin[p,i], S. MacMullin[p,i], R.D. Martin[j], S. Meijer[p,i], S. Mertens[b], M. Nomachi[o], J.L. Orrell[c], C. O'Shaughnessy[p,i], N.R. Overman[c], D.G. Phillips II[l,i], A.W.P. Poon[b], K. Pushkin[j], D.C. Radford[a], J. Rager[p,i], K. Rielage[f], R.G.H. Robertson[m], E. Romero-Romero[n,a], M.C. Ronquest[f], A.G. Schubert[m], B. Shanks[p,i], T. Shima[o], M. Shirchenko[g], K.J. Snavely[p,i], N. Snyder[j], A.M. Suriano[k], J. Thompson[r,k], V. Timkin[g], W. Tornow[h,i], J.E. Trimble[p,i], R.L. Varner[a], S. Vasilyev[n], K. Vetter[b,2], K. Vorren[p,i], B.R. White[a], J.F. Wilkerson[p,i,a], C. Wiseman[d], W. Xu[f], E. Yakushev[g], A.R. Young[l,i], C.-H. Yu[a], V. Yumatov[e]

[a] *Oak Ridge National Laboratory, Oak Ridge, TN, USA*
[b] *Nuclear Science Division, Lawrence Berkeley National Laboratory, Berkeley, CA, USA*
[c] *Pacific Northwest National Laboratory, Richland, WA, USA*
[d] *Department of Physics and Astronomy, University of South Carolina, Columbia, SC, USA*
[e] *Institute for Theoretical and Experimental Physics, Moscow, Russia*
[f] *Los Alamos National Laboratory, Los Alamos, NM, USA*
[g] *Joint Institute for Nuclear Research, Dubna, Russia*
[h] *Department of Physics, Duke University, Durham, NC, USA*
[i] *Triangle Universities Nuclear Laboratory, Durham, NC, USA*
[j] *Department of Physics, University of South Dakota, Vermillion, SD, USA*
[k] *South Dakota School of Mines and Technology, Rapid City, SD, USA*
[l] *Department of Physics, North Carolina State University, Raleigh, NC, USA*
[m] *Center for Experimental Nuclear Physics and Astrophysics, and Department of Physics, University of Washington, Seattle, WA, USA*
[n] *Department of Physics and Astronomy, University of Tennessee, Knoxville, TN, USA*
[o] *Research Center for Nuclear Physics and Department of Physics, Osaka University, Ibaraki, Osaka, Japan*
[p] *Department of Physics and Astronomy, University of North Carolina, Chapel Hill, NC, USA*
[q] *Centre for Particle Physics, University of Alberta, Edmonton, AB, Canada*
[r] *Department of Physics, Black Hills State University, Spearfish, SD, USA*
[s] *Tennessee Tech University, Cookeville, TN, USA*

[1] Permanent address: Tuebingen University, Tuebingen, Germany
[2] Alternate Address: Department of Nuclear Engineering, University of California, Berkeley, CA, USA

Selection and peer review is the responsibility of the Conference lead organizers, Frank Avignone, University of South Carolina, and Wick Haxton, University of California, Berkeley, and Lawrence Berkeley Laboratory
doi:10.1016/j.phpro.2014.12.038

[t]Shanghai Jiao Tong University, Shanghai, China

Abstract

The MAJORANA DEMONSTRATOR will search for neutrinoless-double-beta decay ($0\nu\beta\beta$) in ^{76}Ge, while establishing the feasibility of a future tonne-scale germanium-based $0\nu\beta\beta$ experiment, and performing searches for new physics beyond the Standard Model. The experiment, currently under construction at the Sanford Underground Research Facility in Lead, SD, will consist of a pair of modular high-purity germanium detector arrays housed inside of a compact copper, lead, and polyethylene shield. Through a combination of strict materials qualifications and assay, low-background design, and powerful background rejection techniques, the DEMONSTRATOR aims to achieve a background rate in the $0\nu\beta\beta$ region of interest (ROI) of no more than 3 counts in the $0\nu\beta\beta$-decay ROI per tonne of target isotope per year (cnts/(ROI-t-y)). The current status of the DEMONSTRATOR is discussed, as are plans for its completion.

Selection and peer review is the responsibility of the Conference lead organizers, Frank Avignone, University of South Carolina, and Wick Haxton, University of California, Berkeley, and Lawrence Berkeley Laboratory

Keywords: neutrinoless double beta decay, germanium detector, majorana
PACS: 23.40.-2

1. Introduction

Neutrinoless-double-beta decay ($0\nu\beta\beta$) is a lepton-number violating, second-order weak interaction which requires neutrinos to be Majorana particles (indistinguishable from their anti-particles) in order to proceed [1][2]. Majorana neutrinos can provide an explanation for the mass discrepancy between the neutrinos and the charged fermions of the Standard Model via the so-called "seesaw" mechanism [3][4][5][6], and for the preponderance of matter over anti-matter through leptogenisis [7][8]. $0\nu\beta\beta$ experiments can probe the absolute mass scale of the neutrino, and potentially distinguish between the normal and inverted neutrino mass hierarchies. $0\nu\beta\beta$ searches are at the forefront of ultra-rare event detection; recent experimental lower limits of $T^{0\nu}_{1/2}$ are greater than 10^{25} years. Future experiments seek sensitivity to lifetimes greater than 10^{27}years, requiring tonnes of source material, years of observation time, and near-zero background [9].

2. DEMONSTRATOR Experimental Overview

Germanium detectors have been and remain an attractive option for $0\nu\beta\beta$-decay experiments, in which germanium diodes fabricated from mass-76-enriched germanium serve as source and detector. ^{76}Ge has a relatively favorable nuclear matrix element according to shell model and QRPA estimations [10], and a well-understood enrichment processes. Germanium detectors have very good energy resolution, important for elimination of background events, and sophisticated event reconstruction techniques have been developed for further background rejection.

The MAJORANA Collaboration is building the MAJORANA DEMONSTRATOR [11] to search for $0\nu\beta\beta$-decay in modular arrays of ^{76}Ge-enriched detectors and to address the following scientific and technical goals:

- Demonstrate a path forward to achieve a background rate at or below 1cnt/(ROI-t-y) in the 4 keV region of interest (ROI) around the 2039 keV Q-value for $0\nu\beta\beta$-decay. This is required for tonne-scale germanium-based searches that will probe the inverted hierarchy parameter space for $0\nu\beta\beta$-decay.
- Show technical and engineering scalability toward a tonne-scale instrument.
- Test the Klapdor-Kleingrothaus claim of observation of $0\nu\beta\beta$ [12].
- Perform searches for physics beyond the standard model, such as the search for dark matter and axions.

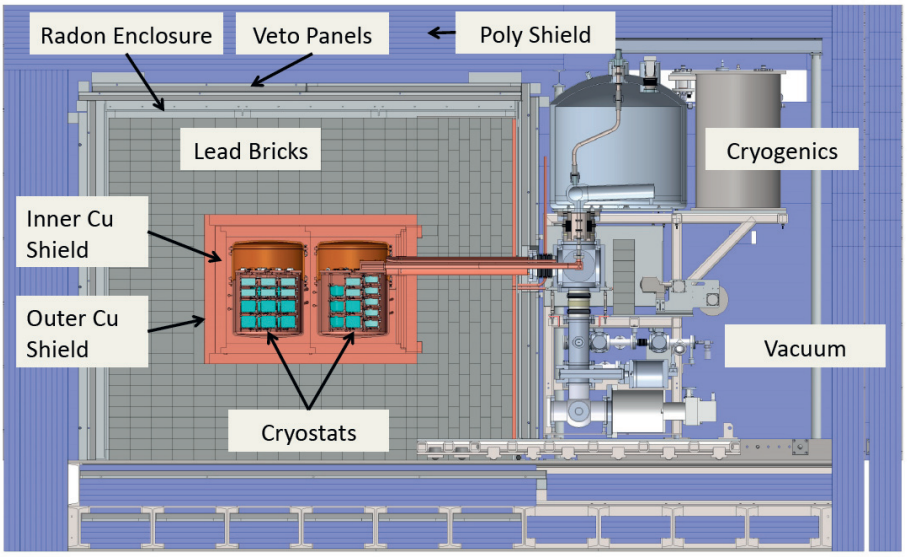

Fig. 1. The Majorana Demonstrator consists of a pair of modular arrays of enriched germanium detectors housed in a layered compact shield of copper, lead, and polyethylene. Each cryostat module is equipped with its own independent vacuum and cryogenic systems. A low-radon environment is created by purging an enclosure surrounding the lead shield, and a 4π active muon veto system surrounds the shield as well.

To probe the majorana mass region allowed by the inverted hierarchy, a future tonne-scale experiment will require ^{76}Ge $T^{0\nu}_{1/2}$ sensitivity greater than 10^{27} years. This will require construction of a detector with several tonne-years of exposure that has background events sufficiently suppressed so as to rate fewer than 1 count in the $0\nu\beta\beta$-decay ROI per tonne of target isotope per year. The primary technical goal of the Majorana Demonstrator is to show that it is feasible to construct a tonne-scale germanium-based experiment, while constraining backgrounds to ∼1cnt/(ROI-t-y), about 100 times lower than that which has been achieved in previous experiments.

The Demonstrator is shown, in section view, in Figure 1. 40 kg of germanium detectors, 30 kg of which are enriched to 86% in ^{76}Ge, are housed within two separate cryostats constructed from ultra-low-background electroformed copper. The cryostats are surrounded by 5 cm of electroformed copper shielding, and 5 cm of commercially-sourced copper. A stacked-brick lead shield 45 cm thick surrounds the copper on all sides. Aluminum panels enclose the lead stack, and serve as the outer boundary of a radon-exclusion zone into which is fed a supply of radon-mitigated nitrogen gas. A plastic scintillator muon veto surrounds the lead shielding, and 30 cm of polyethylene neutron absorber is the outermost shielding layer. To mitigate backgrounds from cosmic rays and prevent cosmogenic activation of detectors and materials, the experiment is being deployed at 4850 ft depth (4260 m.w.e. overburden) at the Sanford Underground Research Facility in Lead, SD

3. Germanium Detectors for $0\nu\beta\beta$

The Majorana Collaboration has chosen the p-type point contact (PPC) configuration for the germanium detectors in the Demonstrator. PPCs differ from the standard “coaxial” germanium detector configuration in that instead of a central bore-hole contact, the PPCs have a small (few mm radius) deposited or implanted contact. While these detectors retain the excellent energy resolution of the coaxially-configured detectors, PPCs have several performance advantages. First, charge depositions in PPC detectors have a significantly wider range of drift times (up to ∼1 μsec), as compared to coaxial detectors. This allows for significantly improved discrimination and rejection of multi-site events (such as compton-scattering γs) from the single-site $0\nu\beta\beta$ signal through Pulse Shape Analysis (PSA) [13][14]. Second, the small point-contact yields a low overall detector capacitance (∼1 pF). This low capacitance reduces noise, improving

energy resolution at low energy and reducing the energy threshold; energy thresholds below 0.5keV have been realized in these types of detectors [15]. The improved low-energy performance allows for effective rejection of ^{68}Ga positron emission through tagging of the low energy K-shell (10 keV) and L-shell (1 keV) ^{68}Ge X-rays which precede them. It also allows for searches for new physics (e.g. Dark Matter, Axions) in an energy regime inaccessible to other detector technologies. Finally, the rather simple readout scheme afforded by PPCs (1 channel per detector) allows for scaling to larger mass without overwhelming data acquisition needs.

The Demonstrator is being built around a combination of germanium detectors enriched in ^{76}Ge, and detectors produced from un-enriched (7.6% natural abundance) germanium material. 41.6 kg of enriched material has been supplied to AMETEK/ORTEC for the fabrication of PPC detectors, from which 30 kg of PPC detectors are expected to be fabricated, each with a mass of around 1 kg. At the time of this writing, 26 of these detectors have been fabricated, delivered, and tested by the collaboration for suitability. A scheduled delivery in April, 2014 will bring the total to 25 kg of enriched detectors, and another 4-5 kg are expected by October. The collaboration is in possession of 20 kg of natural detectors which will comprise the remaining detector mass. These detectors are modified BEGe detectors from CANBERRA Industries, each with a mass typically in the 600-700 g range, and which do not include the typical thin front window that allows the unmodified BEGes to be sensitive to low-energy γ-rays. Both enriched and natural detectors are stored underground prior to installation to limit cosmogenic production of ^{68}Ge.

4. Materials Production and Qualification

The Demonstrator's unprecedented background requirements demand careful scrutiny of all materials used in detector construction. Radiopurity assays are performed on candidate materials using Neutron Activation Analysis (NAA), Inductively-Coupled Plasma Mass Spectrometry (ICP-MS), and direct γ-ray counting. Assay results are combined with simulation to estimate background contributions from materials, and set upper limits on acceptable impurity content and component masses.

The workhorse material from which the majority of inner components are fabricated is copper that has been manufactured by the Majorana Collaboration itself. Electroforming is an electrochemical process by which copper feedstock is dissolved into an electrolyte solution, then plated onto a metallic mandrel through the application of a bias potential. It had been shown that through this electroforming process it is possible to produce copper which has a radio-impurity content of 0.17 μBq ^{238}U/kg Cu, and 0.06 μBq ^{232}Th/kg Cu [16], and has excellent mechanical properties [17]. It is, however a time-consuming process; a 1.25-cm-thick volume, suitable for use in fabricating cryostat components and shielding material, can take as long as 8-12 months to complete.

While the electroforming process will produce very pure material, it cannot prevent subsequent activation of the bulk by cosmic rays. In order to limit production of cosmogenic impurities, ^{60}Co in particular, the electroforming process is performed underground at SURF, in a clean room facility constructed for this purpose. A fully-outfitted underground machine shop was assembled in the Demonstrator's clean room laboratory for the fabrication of components from the bulk material, and a chemical processing station was assembled for surface cleaning and treatment of the completed parts. As a result copper parts are never brought to the surface, with the exception of a few parts which require electron-beam welding at an off-site location or parylene plastic coating on the surface at SURF.

For the electrical insulators required in constructing PPC detector mounts, a single lot of acid-leached NXT-85 (a PTFE variant) serves as the source material. Vespel SP-1 is used sparingly where its mechanical properties are required in mechanical supports and electrical connectors. Parylene plastic is used as a coating to prevent seizure of threaded copper components, and as a gasket material as described in the following section.

5. Modular Germanium Detector Arrays

Germanium detectors are typically operated at liquid nitrogen temperature to suppress thermal production of electron-hole pairs, and in a high-vacuum environments for thermal isolation and prevention

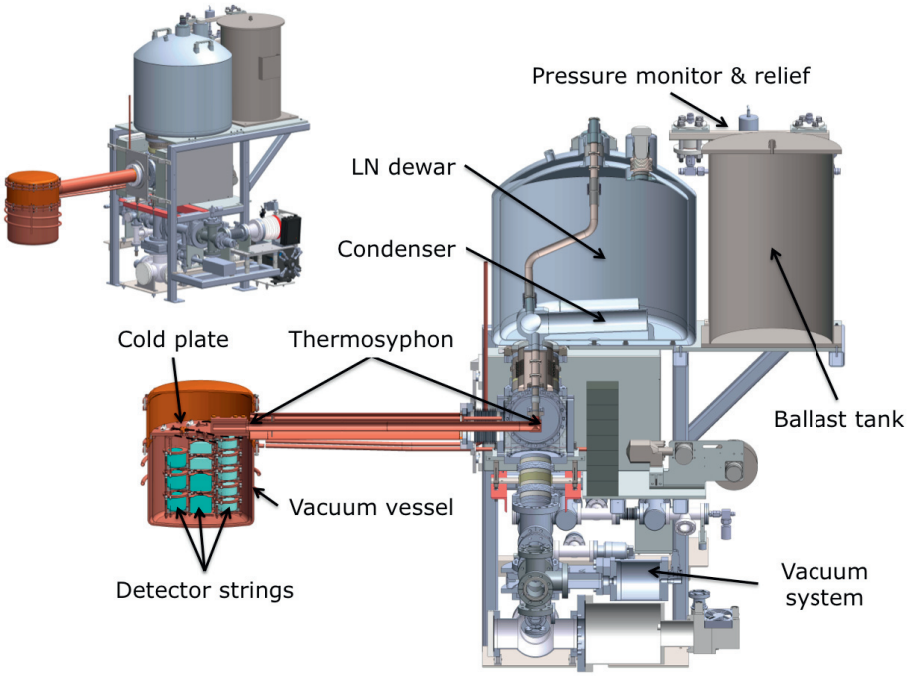

Fig. 2. The detectors of the MAJORANA DEMONSTRATOR are housed in a pair of copper vacuum cryostats, each with its own vacuum and cryogenic systems. These "modules" allow for phased detector deployment, and suggest a natural scheme for scalability to a larger experiment.

cryogenic adsorption of material onto sensitive passivated germanium surfaces between charge-collection and bias voltage contacts. The DEMONSTRATOR's detectors are being deployed in a pair of copper vacuum cryostats, each independently operating as a stand-alone "module." Detectors are mounted in individual low-mass copper and PTFE "detector unit" assemblies. The detector units are designed to rigidly support the detector, house the front-end electronics, and provide solid electrical contact to charge collection and detector bias electrodes through temperature cycles from room-temperature to 80 K. Minimization of radioactive backgrounds from bulk contaminants in the copper and PTFE plastic used in the construction of the detector units require using the minimal mass of copper which will fulfill the structural requirements, and using the minimal mass of PTFE required for electrical isolation. Assembled detector units are are then stacked into "strings" of 4-5 detectors apiece, dependent upon the lengths of the installed detectors. Seven strings are then deployed in each module.

The vacuum cryostats are constructed from ultra-low-background electroformed copper, due to the strict radio-purity requirements for materials used in the demonstrator. Cylindrical vessel components are bolted and sealed together following detector installation, and a welded "cross-arm tube" provides the vacuum pumping and cable routing path through the shielding stack. As background constraints prohibit the use of elastomers typically used as gaskets or o-rings, a new seal technology was developed for use in the demonstrator in which a thin ($\sim$1 μm) sheet of Parylene plastic is used as a combination of gasket and lubricating material between two tapered faces machined into the mating copper parts. Outside of the copper and lead shielding, a transition is made to standard stainless-steel UHV-grade vacuum hardware. Each cryostat is fitted with its own vacuum system, equipped with a 3.3 lps oil-free diaphragm roughing pump, 300 lps magnetically levitated turbo-molecular pump, and 1200 lps, 10 K cryopump. The system is completely remotely-operable, a necessity for deployment in an underground location where access may be periodically restricted.

Cooling of the detector arrays is accomplished through the use of a thermosyphon-based system, as shown in Figure 2 [18]. A hollow copper thermosyphon tube runs coaxially with and internal to the cross-

arm tube. A fixed nitrogen gas supply is condensed inside of a custom-fabricated liquid nitrogen dewar, and flows as a thin layer of liquid to the cold plate to which the detector strings are mounted. Heat is drawn out of the cold plate, evaporating the nitrogen in the thermosyphon, whereupon it flows back to the condenser. Adjustment of the initial nitrogen mass load inside of the thermosyphon system modifies the volume of liquid nitrogen flow, and the effective thermal conductance of the thermosyphon system. Use of a fixed nitrogen load prevents introduction of radon into the shielded volume, and keeping the nitrogen layer thin should limit microphonic noise. Additionally, use of a liquid cryogen as a thermal conductor allows for electrical isolation of the cryostat system from the primary cooling source (liquid nitrogen dewar) through the use of a vacuum electrical break.

At the time of writing, the Majorana Collaboration is commissioning a "Prototype Module", which has served as a testbed for Demonstrator mechanical design, fabrication processes, and assembly procedures. The cryostat of the Prototype Module was fabricated from commercially-sourced copper, as commercial material is significantly less expensive and more rapidly obtained than underground electroformed material. Two strings of natural germanium detectors have been installed in the Prototype Module, and significant improvements to detector cabling and connectors and cryostat IR shielding have been made as a result of assembly and testing. Due to delays in obtaining a custom dewar for thermosyphon operation, the Prototype Module is cooled using a 60 W pulse-tube cooler, and temperature stabilized using installed temperature sensors and cartridge heaters in a closed-loop PID feedback loop. This has allowed for precise temperature control and variability over a wide range (50-100 K) during commissioning.

While commissioning the Prototype Module, fabrication and assembly of the two production Modules produced from underground electroformed copper is ongoing. Nearly all of the copper required for fabrication has been produced, and the majority of the required components have been fabricated. The Majorana Collaboration predicts the commissioning of the first production Module, with enriched detectors, to begin in the summer of 2014, with commissioning of the 2nd Module to begin early in 2015.

6. Passive Shielding and Active Muon Veto

When the modules are fully-populated and ready for deployment, they are transported by air bearing transporter to the pre-assembled lead and copper shield, where they roll on a bearing-equipped platform off of the transport and into position in the shield. Figure 3 shows the status of the lead and copper shield at the time of writing. A 5-cm-thick box constructed from commercially sourced copper is in place, supported from below by copper legs so as to be free-standing. 45 cm of lead shielding has been stacked on all sides from 5 cm x 10 cm x 20 cm bricks that have been cleaned and etched to remove oxide and surface contaminants. As γ-rays emitted by the innermost shielding can contribute to background, 5 cm of ultra-pure electoformed copper will comprise the inner layer of shielding. This inner copper shield is not shown in Figure 3; an inner box constructed from 1.25-cm-plates will be inserted prior to detector deployment. Openings have been left in the copper and lead shield for the installation of the populated cryostats; the copper and lead required to complete the shield at the openings will be pre-installed on ball-bearing tables prior to insertion of the modules.

The lead and copper shield is surrounded by a set of aluminum panels creating a nearly hermetic volume into which nitrogen gas can be supplied to form a low radon environment. The nitrogen gas is generated by boiling liquid nitrogen, further scrubbed with a cooled charcoal trap, and monitored with an electrostatic chamber. Currently, the panels of the radon exclusion box have been fabricated and are awaiting installation; the purge gas supply system is nearing completion.

Two layers of scintillating acrylic panels, each 2.54 cm thick, will be installed immediately outside of the radon exclusion box to create an active muon veto with 4π coverage. The scintillator is fitted with wavelength-shifting fibers embedded in longitudinal grooves, and the assembly is wrapped in reflective material. The fibers from a single panel are bundled, and light is detected via a 1.27 cm photomultiplier tube. The assembly is then encapsulated in an aluminum enclosure. Of the 32 veto panels, 12 have been assembled and installed, and the remaining 20 are ready for installation.

The outermost layer of shielding in the Demonstrator is neutron absorber constructed from high-density polyethylene (HDPE). 2.54-cm-thick sheets are stacked to form an HDPE layer 30 cm in thickness, the inner

Fig. 3. A photograph of the status of the passive shield assembly, at the time of writing. The outer half of the copper shield, 5-cm-thick and fabricated from commercial copper, forms a box in the center of the shielding. It is surrounded by 45 cm of stacked lead bricks. An inner copper shield fabricated from ultra-pure electroformed copper, veto panels, and polyethylene shield remain to be installed.

5 cm of which are made from borated HDPE. Fabrication of the HDPE panels is ∼15% complete at the time of writing.

7. Data Acquisition Electronics and Software

The signal-readout of the PPC detectors of the Demonstrator is accomplished through a low-noise, low-radioactivity resistive feedback circuit. A low-mass front end (LMFE) electronics board consisting of the input FET and feedback components bonded to a fused-silica substrate is mounted on the detector unit, ∼10 mm from the point contact, to minimize stray input capacitance [19]. Four 0.4-mm-diameter, 50 Ω coaxial cables, chosen for background and thermal considerations, connect the LMFEs to the preamplifiers, which are housed outside of the shielding at the far end of the cross-arm tube. Each preamplifier is equipped with high-gain and low-gain outputs for separate digitization. The digitizers used in the Demonstrator are 10-input, 100-MHz, 14-bit digitizer boards developed for the GRETINA experiment [20]. An on-board FPGA performs real-time digital signal processing, including discrimination, shaping, and pole-zero correction. Separate controller cards are equipped with pulsers capable of sending variable-amplitude pulses to the LMFE FETs, DACs for varying FET drain-to-source voltages, and ADCs for monitoring first-stage outputs of the preamplifiers.

The software used for data acquisition and slow controls throughout the Demonstrator is ORCA (Object-oriented Real-time Control and Acquisition) [21]. ORCA, written in Obj-C using the Cocoa framework and Apple development tools, is a modular, general purpose, graphical framework for experiment data acquisition and control. The data acquisition framework can be modified at run-time to represent different hardware configurations and readout schemes. Hardware components are represented graphically, and can be enabled by dragging them from a hardware catalog into the configuration window; data flow is represented by interconnects between the graphical objects. In addition to the readout of signals from detectors, ORCA is used

to readout signals from the veto system, control the vacuum and cryogenic systems, and monitor laboratory environmental conditions.

The full data acquisition system is currently being commissioned while operating the detectors in the Prototype Module. Efforts are in progress to optimize digitizer performance, and to stress-test the data acquisition chain prior to operation of the full 140-channel readout and digitization system.

8. Background Estimation

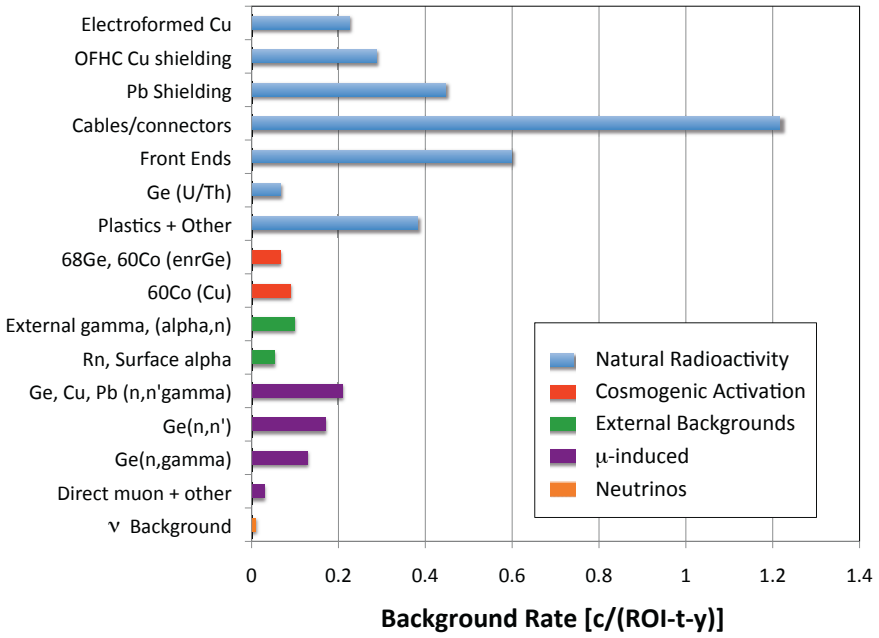

Fig. 4. Summary of sources of background counts in the $0\nu\beta\beta$ ROI. in cnts/(ROI-t-y), based on MaGe simulations of the Demonstrator geometry and current radio-impurity assay results and upper limits. Total $0\nu\beta\beta$ background is estimated at 4.1 cnts/(ROI-t-y)

The background goal set for the Demonstrator is 3 cnts/(ROI-t-y), which the collaboration believes can be extrapolated to 1 cnt/(ROI-t-y) with increased shielding, self-shielding, and potentially increased overburden through deeper deployment. Backgrounds have been estimated through an extensive simulation campaign using MaGe, a Geant4-based simulation framework developed jointly between the Majorana and Gerda collaborations [22]. A high-resolution model of the Demonstrator geometry has been developed for use in MaGe, and a full suite of backgrounds have been simulated, including the full uranium and thorium decay chains, ^{60}Co, ^{40}K, and others. Estimates of effectiveness of background cuts can be made by examining the topology of simulated events, eliminating events which deposit energy in multiple detectors or in sufficiently spacially-separated depositions in a single detector that would be rejected by PSA. Simulated spectra from individual components and decays are combined with estimates of radio-impurity concentrations from assays to predict overall background spectra and rates in the $0\nu\beta\beta$ ROI. The expected contributions to the $0\nu\beta\beta$ ROI, based on assayed impurity concentrations and assay upper limits, are shown in Figure 4, and sum to 4.1 cnts/(ROI-t-y). For a more complete discussion of estimation of backgrounds in the Demonstrator, see C. Cuesta's article *Background Model for the* Majorana Demonstrator in this publication, and references therein.

9. Acknowledgments

We acknowledge support from the Office of Nuclear Physics in the DOE Office of Science, the Particle Astrophysics Program of the National Science Foundation, and the Russian Foundation for Basic Research. We acknowledge the support of the Sanford Underground Research Facility administration and staff.

References

[1] E. Majorana. Teoria simmetrica dell'elettrone e del positrone. *Nuovo Cimento*, 5(4):171–184, 1937.
[2] J. Schechter and J. W. F. Valle. Neutrinoless double-beta decay in su(2)u(1) theories. *Phys. Rev. D*, 25:2951–2954, Jun 1982.
[3] P. Minkowski. $\mu \to e\gamma$ at a rate of one out of 109 muon decays? *Physics Letters B*, 67(4):421 – 428, 1977.
[4] T. Yanagida. Horizontal gauge symmetry and masses of neutrinos. In O. Sawada and A. Sugamoto, editors, *Proceedings of the Workshop on Unified Theory and Baryon Number in the Universe*. KEK, Tsukuba, Japan, 1979.
[5] M. Gell-Mann, P. Ramond, and R. Slansky. *Supergravity*. North- Holland, Amsterdam, The Netherlands, 1979.
[6] R. N. Mohapatra and G Senjanović. Neutrino mass and spontaneous parity nonconservation. *Phys. Rev. Lett.*, 44:912–915, Apr 1980.
[7] M. Fukugita and T. Yanagida. Barygenesis without grand unification. *Physics Letters B*, 174(1):45 – 47, 1986.
[8] P. Di Bari. An introduction to leptogenesis and neutrino properties. *Contemporary Physics*, 53(4):315–338, 2012.
[9] S. R. Elliott and P. Vogel. Double beta decay. *Annual Review of Nuclear and Particle Science*, 52(1):115–151, 2002.
[10] E. Caurier et al. Influence of pairing on the nuclear matrix elements of the neutrinoless decays. *Phys. Rev. Lett.*, 100:052503, Feb 2008.
[11] N. Abgrall et al. The MAJORANA DEMONSTRATOR neutrinoless double-beta decay experiment. *Adv. High Energy Phys.*, 2014, 2014.
[12] H.V. Klapdor-Kleingrothaus and I.V. Krivosheina. The evidence for the observation of $0\nu\beta\beta$ decay: The identification of $0\nu\beta\beta$ events from the full spectra. *Mod.Phys.Lett.*, A21:1547–1566, 2006.
[13] R.J. Cooper et al. A pulse shape analysis technique for the majorana experiment. *Nuclear Instruments and Methods in Physics Research Section A: Accelerators, Spectrometers, Detectors and Associated Equipment*, 629(1):303 – 310, 2011.
[14] D. Budjáš et al. Pulse shape discrimination studies with a broad-energy germanium detector for signal identification and background suppression in the gerda double beta decay experiment. *Journal of Instrumentation*, 4(10):P10007, 2009.
[15] P. S. Barbeau, J. I. Collar, and O. Tench. Large-mass ultralow noise germanium detectors: performance and applications in neutrino and astroparticle physics. *Journal of Cosmology and Astroparticle Physics*, 2007(09):009, 2007.
[16] E.W. Hoppe et al. Determination of method detection limits for trace 232-thorium and 238-uranium in copper using ion exchange and icpms. Technical Report PNNL-23293, Pacific Northwest National Laboratory, Richland, WA, 2014.
[17] N.R. Overman et al. Majorana electroformed copper mechanical analysis. Technical Report PNNL-21315, Pacific Northwest National Laboratory, Richland, WA, 2012.
[18] E. Aguayo et al. The design of an ultra-low background thermosyphon for the majorana demonstrator. *Nuclear Instruments and Methods in Physics Research Section A: Accelerators, Spectrometers, Detectors and Associated Equipment*, 709(0):17 – 21, 2013.
[19] P. Barton et al. Low-noise low-mass front end electronics for low-background physics experiments using germanium detectors. In *Proceedings of the IEEE Nuclear Science and Medical Imaging Conference (NSS/MIC '11)*, pages 1976–1979. Valencia, Spain, 2011.
[20] S. Zimmermann et al. Implementation and performance of the electronics and computing system of the gamma ray energy tracking in-beam nuclear array (gretina). *IEEE Transactions on Nuclear Science*, 59(5):2494–2500, 2012.
[21] M. A. Howe et al. Sudbury neutrino observatory neutral current detector acquisition software overview. *IEEE Transactions on Nuclear Science*, 51(3):878–883, 2004.
[22] M. Boswell et al. Mage- a geant4-based monte carlo application framework for low-background germanium experiments. *IEEE Transactions on Nuclear Science*, 58(3):1212–1220, 2011.